

# Thermal, Thermo-Mechanical, and Dynamic Mechanical Properties of Polypropylene/Cycloolefin Copolymer Blends

Luca Fambri,<sup>1</sup> Jan Kolarik,<sup>2</sup> Alessandro Pegoretti,<sup>1</sup> Amabile Penati<sup>1</sup>

<sup>1</sup>Department of Materials Engineering and Industrial Technologies, University of Trento, 38123 Trento, Italy

<sup>2</sup>Institute of Macromolecular Chemistry, Academy of Sciences of the Czech Republic, 162 06 Prague 6, Czech Republic

Received 29 December 2010; accepted 24 February 2011

DOI 10.1002/app.34426

Published online 12 July 2011 in Wiley Online Library (wileyonlinelibrary.com).

**ABSTRACT:** Interaction of the components and physical properties of the polypropylene (PP)/cycloolefin copolymer (COC) blends were studied by means of differential scanning calorimetry (DSC), dynamic mechanical thermal analysis (DMTA), Vicat softening temperature (VST), and measurements of the coefficient of linear thermal expansion (CLTE) and of the density. The attention was focused on the blends with 90–60% of PP by wt, where the COC minority component was present in the form of short fibers. DSC, DMTA, and density measurements concurrently prove the immiscibility of PP and COC. DSC measurements reveal that crystallinity and melting temperature of the PP component slightly decrease with the fraction of COC in blends, in the range of 56–47% and 164–161°C,

respectively. Storage modulus and loss modulus of the blends are in a good accord with the model predictions based on (i) the equivalent box model (EBM) and on (ii) modified equations of the percolation theory. The dependence of the VST on the blend composition is in a good correlation with the previous morphological analysis. Measurements of the coefficient of thermal expansion provide useful data as the functions of temperature and blend composition. Density of the blends was found to obey the volume additivity. © 2011 Wiley Periodicals, Inc. *J Appl Polym Sci* 122: 3406–3414, 2011

**Key words:** blends; poly(propylene); cycloolefin copolymer; thermal properties

## INTRODUCTION

Preparation of polymer blends is one of the most cost-effective ways of the upgrading of existing polymers. As potential applications of a polymer blend are closely related to its physical properties, it is desirable to study how these properties depend on the blend phase structure (morphology). As generally known, polypropylene (PP) shows relatively low modulus, yield strength, and resistance to creep. Thus, search for “upgrading” components, which could easily be blended with PP, is still an interesting issue. Amorphous ethylene–norbornene copolymers—usually denoted as cycloolefin copolymers (COCs)—synthesized with metallocene-based catalysts rank among polymer materials with remarkable properties, such as a relatively high glass transition temperature ( $T_g$ ), transparency (the length of ethylene sequences is not sufficient for crystallization), heat resistance, chemical resistance to common solvents, low moisture uptake, high water barrier, good mechanical

properties, etc.<sup>1–3</sup> Rising percentage of norbornene accounts for the increase in yield or tensile strength and decrease in strain at yielding or break (the phenomenon of yielding is preserved up to about 40% of norbornene in copolymers).<sup>4–6</sup> Existing studies of mechanical properties of COC encompass dynamic mechanical thermal analysis (DMTA),<sup>7,8</sup> stress–strain measurements,<sup>4,6,7</sup> flexural creep,<sup>6</sup> micro-hardness,<sup>7</sup> impact strength,<sup>9</sup> creep,<sup>10</sup> and tensile and impact properties.<sup>11</sup>

Preparation of PP blends without compatibilizers is viewed as rather difficult because the compatibility of PP with other polymers is limited.<sup>12</sup> Because of olefinic character,<sup>13,14</sup> COC appears to be easily dispersed in PP and other polyolefins. Particularly, we were able to prepare the PP/COC heterogeneous blends after processing the selected PP and COC polymer without compatibilizers.<sup>15,16</sup> Of available COC products of TOPAS Advanced Polymers, we used Topas 8007, i.e., the copolymer with the lowest fraction of norbornene (about 30%), which displays yielding and relatively high strain at break (10%).<sup>4</sup> Our preliminary microscopy study of the phase structure of the prepared PP/COC blends has shown that injection molded samples with 10–40 wt % of COC include short fibers of COC uniaxially oriented in the direction of injection.<sup>15</sup> In the 90/10, 80/20, and 70/30 blends, the PP matrix contained fibers of COC, whose average diameter increased

Correspondence to: L. Fambri (luca.fambri@ing.unitn.it).

Contract grant sponsor: The second author (J. K.) is greatly indebted to the Grant Agency of the Czech Republic for financial support making the participation in this work possible (Grant No. 106/09/1348).

**TABLE I**  
Glass Transition Temperature, Melting, and Crystallization Data of the PP/COC Blends as Function of Weight Composition

PP/COC <sup>a</sup>	First heating			Cooling		Second heating			$T_{g1}^i$ (°C)	$T_{g2}^i$ (°C)
	$T_{g2}^b$ (°C)	$T_{m1}^c$ (°C)	$C_1^d$ (%)	$T_{c1}^e$ (°C)	$C_1^f$ (%)	$T_{g2}^b$ (°C)	$T_{m1}^c$ (°C)	$C_1^d$ (%)		
100/0	—	163.7	56.0	108.8	61.5	—	160.6	61.7	9.6	—
95/05	75.3	163.9	56.0	113.5	61.5	n.d. <sup>g</sup>	159.8	61.1	8.9	80.4
90/10	74.0	163.4	56.1	114.2	61.3	76.2	159.4	60.6	7.9	80.2
85/15	73.4	163.1	55.2	112.1	60.7	n.d. <sup>g</sup>	160.0	60.3	7.1	79.9
80/20	74.3	162.9	55.3	113.2	61.2	76.3	159.8	61.0	7.8	80.6
75/25	75.3	163.0	54.6	112.2	60.6	75.3	158.9	60.6	7.3	81.2
70/30	74.3	163.0	54.8	113.2	60.0	75.4	158.0	59.3	7.9	80.1
60/40	75.4	163.2	55.6	112.7	60.3	76.4	159.1	60.0	7.2	79.8
50/50	74.6	162.7	53.9	111.0	57.3	77.6	159.7	59.1	8.1	80.7
25/75	73.4	160.9	47.3	103.2 <sup>h</sup>	54.1	76.4	159.9	54.3	8.1	80.7
0/100	74.5	—	—	—	—	78.5	—	—	—	81.0

<sup>a</sup> Blend composition by wt %.

<sup>b</sup> Glass transition temperature of COC detected by DSC measured in the first or in the second heating scan.

<sup>c</sup> Melting temperature of PP component measured in the first or in the second heating scan.

<sup>d</sup> Normalized crystallinity of PP component measured in the first or in the second heating scan.

<sup>e</sup> Crystallization temperature of PP component in the cooling scan.

<sup>f</sup> Normalized crystallinity of PP component during the cooling scan.

<sup>g</sup> Not detectable.

<sup>h</sup> Shoulder peak at 108.5°C.

<sup>i</sup> Glass transition temperature of PP and COC measured at the maximum of loss modulus by DMTA.

with COC fraction in the range 0.25–0.80  $\mu\text{m}$ . In the 60/40 blend, COC component formed both fibers (average diameter 2.6  $\mu\text{m}$ ) and larger elongated entities embedded in the PP matrix. The 50/50 blend consisted of cocontinuous COC with PP components. Microphotographs of fracture surfaces have revealed that most COC fibers were partly pulled out from the PP matrix, but some were broken, which evidences rather mediocre interface adhesion between PP and COC. With regard to the micrographs<sup>15</sup> and mechanical properties<sup>10,11</sup> of the blends, the fiber aspect ratio was estimated to exceed 20. Rheology of the PP/COC blends was briefly described in our previous article.<sup>16</sup> As the fibrous morphology of blends prepared by a single-step technique is an interesting phenomenon sometimes observed in oriented immiscible blends,<sup>17–24</sup> these PP/COC blends appear to be materials worth of more detailed and deeper studies. The objective of this research is to estimate the effects of the blend composition on thermal properties, density, dynamic mechanical and thermomechanical properties, and dilatation.

## EXPERIMENTAL

### Materials

Polypropylene Moplen C30G was a product of Lyondell-Basell, Ferrara, Italy: melt flow index (MFI; 230°C, 2.16 kg) =  $5.7 \pm 0.1$  dg/min; density: 0.90 g/cm<sup>3</sup>; crystallinity: 45%. An amorphous COC produced under the trade name Topas 8007 was a product of TOPAS

Advanced Polymers, Germany, consisting of 30% of bicyclo(2.2.1)hept-2-ene (norbornene) units and 70% of ethylene units<sup>4</sup>: MFI (230°C, 2.16 kg) =  $11.3 \pm 0.6$  dg/min<sup>1</sup>; density: 1.0 g/cm<sup>3</sup>;  $T_g = 80^\circ\text{C}$ .

### Blend preparation

A series of PP/COC blends was prepared with 5, 10, 15, 20, 25, 30, 40, 50, and 75 wt % of COC (Table I). Polymers were mixed in a Banbury mixer (chamber 4.3 L; 164 rpm) at 190°C for 3.5 min. Produced pellets were used for feeding a Negri-Bossi injection molding machine. Two types of test pieces were prepared: (1) American Society for Testing and Materials (ASTM) D638 (length: 210 mm; thickness: 3.3 mm; gauge length: 80 mm; gauge width: 12.8 mm; melt temperature: 242°C; injection pressure: 20 MPa; mold temperature: 60°C) and (2) ISO 527 (170 mm; 4 mm; 80 mm; 10 mm; 230°C; 30 MPa; 50°C).

### Morphology

Morphology of the selected PP/COC blends was evidenced through Scanning Electron Microscopy (SEM) images on cryofractured surfaces of pre-notched ISO samples, taken by using a Cambridge Stereoscan 200 at an acceleration voltage of about 15 kV, after gold sputtering metallization. The mutual dispersion of each component and the interface at correspondent composition 75/25 and 25/75 were compared.

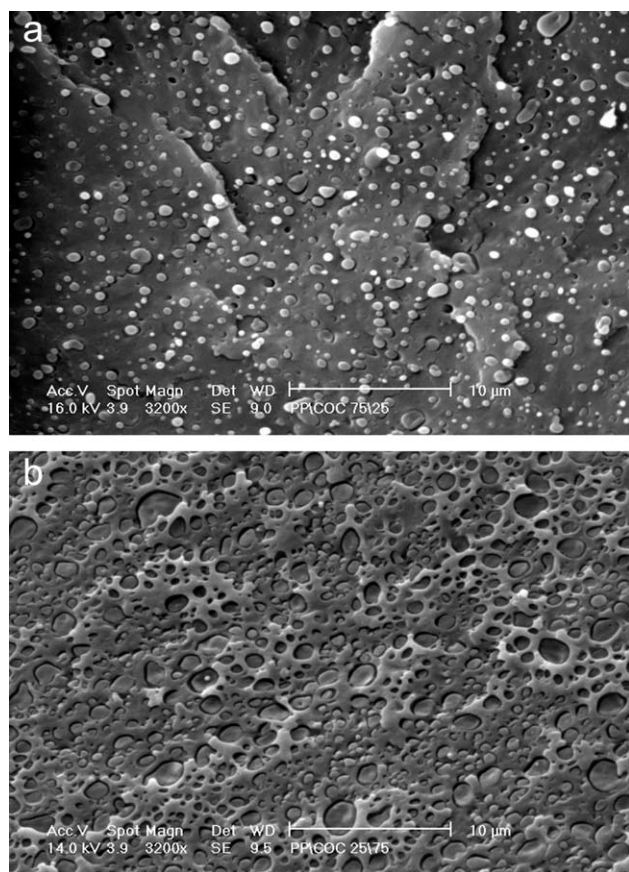


**Figure 1** SEM micrographs of blends PP/COC = 75/25 (a) and PP/COC = 25/75 (b), containing PP at selected weight fraction  $w_1 = 0.75$  and  $w_1 = 0.25$ , respectively.

### Differential scanning calorimetry

Mettler DSC 30 was used to perform two scans in the interval from  $-50$  to  $200^\circ\text{C}$ . The heating rate and the cooling rate (between the scans) were  $10^\circ\text{C}/\text{min}$ . Tests were run under the nitrogen atmosphere (flux:  $100\text{ mL}/\text{min}$ ). Test specimens (about  $20\text{ mg}$ ) were cut from the central part of ASTM test pieces. The measurements provided data on the glass transition temperature  $T_{g2}$  of the COC component (inflection point corresponding to the glass transition temperature  $T_{g1}$  of PP was rather unclear due to PP crystallinity), the melting temperature  $T_{m1}$ , and the melting enthalpy  $\Delta H_{mb}$  of PP in blends. The crystallinity of the PP component (Table I) is calculated as  $C_1 = 100 w_1 \Delta H_{mb} / \Delta H_{m10}$ , where  $w_1$  is the weight fraction of PP in the blends and  $\Delta H_{m10} = 165\text{ J}/\text{g}$  is the melting enthalpy of the crystalline phase of PP.<sup>25</sup>

### Density measurements

Density measurements were carried out according to the method of double weighing following the ASTM D792-08 standard, where ethanol (99.8%) was used as a reference liquid at  $22^\circ\text{C}$ . Three test coupons

(about  $0.7\text{ g}$ ) of each blend were cut from central part of the ASTM specimens.

### Dynamic mechanical thermal analysis

Measurements were performed by using a DMTA Mk II (Polymer Laboratories Ltd., Loughborough, UK). The storage  $E'$  and loss  $E''$  moduli were measured in the single cantilever bending mode at frequency  $1\text{ Hz}$  in the range  $-100$  to  $150^\circ\text{C}$  (test pieces  $12\text{ mm} \times 12.8\text{ mm} \times 3.3\text{ mm}$  were cut of the ASTM specimens; heating rate  $3^\circ\text{C}/\text{min}$ ; dynamic displacement  $0.064\text{ mm}$ ). The glass transition temperature of the PP or COC component was identified with the position of the maximum of the respective loss modulus peak on temperature scale.

The coefficient of (linear) thermal expansion (CLTE) was evaluated by means of the DMTA tensile measurements (specimens  $18\text{ mm} \times 10\text{ mm} \times 4.0\text{ mm}$  were prepared from the ISO pieces; static stress:  $0.025\text{ MPa}$ ; dynamic displacement:  $0.032\text{ mm}$ ; heating rate:  $3^\circ\text{C}/\text{min}$ ; temperature range:  $-40$  to  $70^\circ\text{C}$ ).  $\text{CLTE} = (\Delta L/L_0)/\Delta T$  was calculated for four different temperature intervals  $\Delta T$  by using the initial specimen length  $L_0$  and the length variation  $\Delta L$  over the selected interval  $\Delta T$ .

### Vicat softening temperature

The Vicat softening temperature (VST) was measured according to ASTM D1525-09 with a load of  $10\text{ N}$  and a heating rate of  $120^\circ\text{C}/\text{h}$  by using an HDT-Vicat apparatus model MP3 (product of ATS-FAAR, Vignate, Italy). The dimensions of test specimens prepared from the ASTM pieces were  $12\text{ mm} \times 12.8\text{ mm} \times 3.3\text{ mm}$ . The reported VST is the average value of three measurements.

## RESULTS AND DISCUSSION

### Morphology

Structure and properties of a blend are predetermined by its composition and respective properties of the parent polymers. However, the properties of the blend components may differ from the properties of the starting polymers due to their partial miscibility and changes in their structure (e.g., crystallinity). Figure 1(a,b) compares the morphology of the cross section of ISO blend specimens containing the minor component at a weight fraction  $w = 0.25$ , i.e., with PP/COC composition of 75/25 and 25/75, respectively. Figure 1(a) evidences good dispersion of COC and the formation of microfibrils (about  $1\text{ }\mu\text{m}$  diameter) in the PP matrix, whereas Figure 1(b) shows PP particles with diameter up to  $2\text{ }\mu\text{m}$  dispersed in the COC matrix. Moreover, the presence

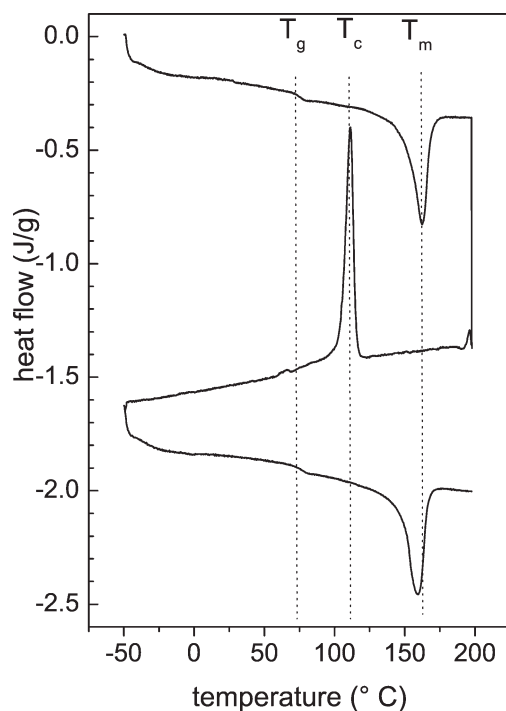


**Figure 2** DSC thermogram of the PP/COC = 50/50 blend. See data in Table I.

of some COC fibers partially pulled out and corresponding cavities in the PP matrix indicate a mediocre interfacial adhesion between the components in 75/25 PP/COC blend.

### Differential scanning calorimetry

Thermograms given in Figure 2 for the 50/50 blend show that amorphous COC displays an inflection localizing its  $T_{g2}$  at about 75°C, whereas  $T_{g1}$  of PP (expected at about 0°C) is difficult to identify owing to PP crystallinity. Table I shows that  $T_{g2}$  of COC is not perceptibly affected by the fraction of PP in the blends, which is documented by differential scanning calorimetry (DSC;  $T_g = 74^\circ\text{C}$ ) and DMTA ( $T_g = 80^\circ\text{C}$ ) measurements. On the other hand, PP exhibits clear-cut melting and crystallization peaks (Fig. 1). Table I indicates a tendency of the PP melting temperature  $T_{m1}$  to slightly decrease with rising fraction of COC in the blends, especially at  $w_1 \leq 0.5$ .

The crystallinity (Table I) of the PP component in as-molded blends decreases proportionally to its weight fraction from about 56% for the neat PP to about 47% for the 25/75 blend. In the second heating scan, the PP crystallinity in the PP-rich blends ( $w_1 \geq 0.5$ ) is almost constant (about 60%) and only slightly lower than that of the neat PP (61.7%). The values of  $\Delta H_{mb}$  registered in the second heating scan are noticeably higher than those in the first scan, which can be ascribed to lower cooling rate (between the first and second heating run) in com-

parison with the cooling rate used in the injection molding of test specimens (higher than 250°C/min). The crystallization temperature  $T_{c1}$  of PP in blends registered in the cooling scan is by 2–5°C higher than that of the neat PP, which might indicate a tiny nucleating effect of COC analogous to that previously observed for the high-density polyethylene (HDPE)/COC blends.<sup>26</sup> The simultaneous drops in the melting temperature, crystallization temperature, and crystallinity for the 25/75 blend indicate that the dominating amorphous COC component inhibits the structural organization of the minority PP component. In particular, the changing morphology of PP dispersed in COC is manifested by an enlargement of the crystallization peak and by a decrease in the crystallization temperature (from about 112 to 103°C). Moreover, a shoulder at 108°C evidences the occurrence of the so-called fractionated crystallization. This phenomenon reviewed by Frensch et al.<sup>27</sup> was recently observed in heterogeneous blends with majority amorphous component, such as polystyrene,<sup>28</sup> polycarbonate,<sup>29</sup> or COC,<sup>30</sup> where minority PP (up to about 30%) exhibited a delayed crystallization at a larger undercooling owing to decreasing particle size.

The melting enthalpy of PP in blends,  $\Delta H_{mb}$ , is not linearly proportional to its weight fraction but is somewhat lower (Fig. 3). Experimental data for

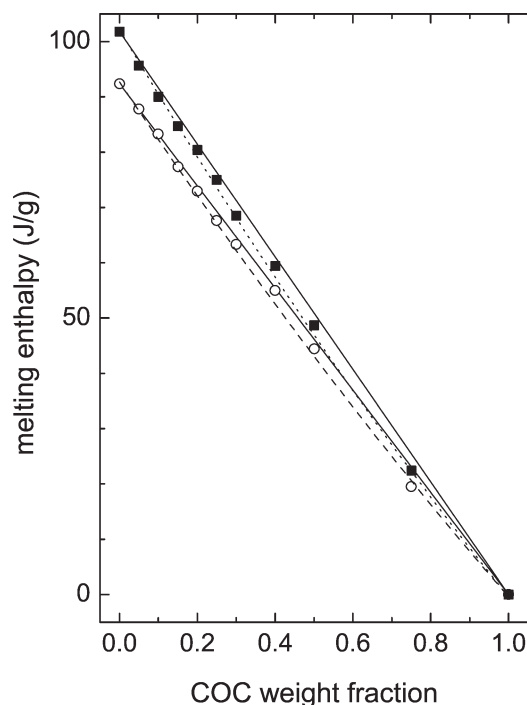


**Figure 3** The melting enthalpy of the PP component in the PP/COC blends. Experimental data: first heating scan (●); second heating scan (■). Parameters of eq. (1) with  $\Delta H_{m2} = 0$ : first heating scan (dashed line):  $P_1 = 0.13$ ,  $\Delta H_{m1} = 92.4$  J/g; second heating scan (dotted line):  $P_1 = 0.15$ ,  $\Delta H_{m1} = 101.8$  J/g; full lines: additivity.

**TABLE II**  
**Volume Fraction, Experimental, and Calculated Density of the PP/COC Blends as Function of Weight Composition**

PP/COC <sup>a</sup>	Volume fraction <sup>b</sup>			$\rho_{PP/COC}$ experimental data (g/cm <sup>3</sup> )	$\rho_{PP/COC}$ calculated values (g/cm <sup>3</sup> ) <sup>c</sup>
	$v_{COC}$	$v_{cPP}$	$v_{aPP}$		
100/0	0.000	0.535	0.465	0.9045 ± 0.0003	0.9017
95/05	0.045	0.511	0.444	0.9092 ± 0.0004	0.9063
90/10	0.091	0.488	0.421	0.9128 ± 0.0005	0.9110
85/15	0.137	0.455	0.408	0.9181 ± 0.0004	0.9150
80/20	0.183	0.432	0.385	0.9223 ± 0.0002	0.9199
75/25	0.230	0.401	0.369	0.9277 ± 0.0009	0.9242
70/30	0.278	0.378	0.344	0.9319 ± 0.0003	0.9293
60/40	0.374	0.332	0.293	0.9412 ± 0.0002	0.9397
50/50	0.473	0.271	0.256	0.9513 ± 0.0007	0.9490
25/75	0.728	0.122	0.150	0.9759 ± 0.0004	0.9740
0/100	1.000	0.000	0.000	1.0040 ± 0.0002	1.0040

<sup>a</sup> Blend composition by wt %.

<sup>b</sup> Volume fraction of COC, crystalline PP, and amorphous PP in the blends, evaluated from composition and experimental crystallinity, considering 1.004, 0.943, and 0.854 g/cm<sup>3</sup> the density of COC, and crystalline and amorphous PP.

<sup>c</sup> Calculated density of PP/COC injection moulded samples.

blends consisting of two crystalline polymers that can be fitted by the following empirical equation recently applied by the authors.<sup>31</sup>

$$\Delta H_{mb} = H_{m1} w_1(1 - P_1 w_2) + H_{m2} w_2(1 - P_2 w_1) \quad (1)$$

where  $w_1$  and  $w_2$  are the weight fractions,  $\Delta H_{m1}$  and  $\Delta H_{m2}$  are the melting enthalpies of the neat components, and  $P_1$  or  $P_2$  are empirical parameters encompassing a negative effect of component 2 on the crystallinity of component 1 and *vice versa*. As COC does not crystallize, the term comprising  $\Delta H_{m2}$  equals to zero for the PP/COC blends. The value of  $P_1 = 0.13$  was obtained for the first heating scan performed with as-molded specimens characterized by  $\Delta H_{m1} = 92.4$  J/g for PP. It is worth noting that the negative deviation of the polyolefin crystallinity was previously observed by the authors also for the HDPE/COC blends.<sup>26</sup>

On the contrary, a positive deviation from eq. (1) has been recently reported for linear low-density polyethylene (LLDPE)/COC blends obtained by melt mixing and compression molding.<sup>32</sup> The values  $\Delta H_{mb}$  observed in the second heating scan deviate more from a straight line, i.e.,  $P_1 = 0.15$  ( $\Delta H_{m1} = 101.8$  J/g), than those found for the first heating scan. As the deviation of the data points from a linear dependence is higher for the blends after melting and crystallization (the second DSC scan), it seems that higher crystallinity of the PP component is accompanied by augmentation of imperfections in the crystalline phase.

## Density

Experimental density of the blends exhibits a linear dependence on the blend composition, as shown in

Table II. The volume fractions of COC ( $v_{COC}$ ), crystalline phase of PP ( $v_{cPP}$ ), and amorphous phase of PP ( $v_{aPP}$ ) in the blends were calculated from the weight composition and melting data in Table I, and the experimental density of COC ( $\rho_{COC} = 1.0040 \pm 0.0002$  g/cm<sup>3</sup>), the literature value of the crystalline PP density ( $\rho_{cPP} = 0.943$  g/cm<sup>3</sup>), and the amorphous PP density ( $\rho_{aPP} = 0.854$  g/cm<sup>3</sup>).<sup>33</sup> Assuming the volume additivity, the blend density  $\rho_b$  can be calculated as a function of the blend composition according to eq. (2):

$$\rho_b = v_{COC} \rho_{COC} + v_{cPP} \rho_{cPP} + v_{aPP} \rho_{aPP} \quad (2)$$

It is well evident that the experimental densities of the PP/COC injection molded samples are systematically higher than those calculated and reported in Table II, which is probably caused by the orientation effect in the processing and/or by a partial interaction of amorphous phase at the interface.

## Dynamic mechanic thermal analysis

Dynamic mechanical patterns (Fig. 4) of the PP/COC blends display two prominent loss modulus peaks at about 8 and 80°C, which correspond to the glass transitions of PP and COC indicated at the frequency of 1 Hz. Table I shows that the temperature location of both loss peaks is independent of the blend composition. Thus, DSC and DMTA concurrently confirm that there is no miscibility of PP and COC, because otherwise  $T_{g1}$  and  $T_{g2}$  should increase and decrease, respectively. Loss modulus dependences show regular changes with increasing fraction of COC in blends, whereas the peak at 80°C grows, the peak at 8°C is proportionally reduced. Moreover, loss modulus curves of the blends intersect around

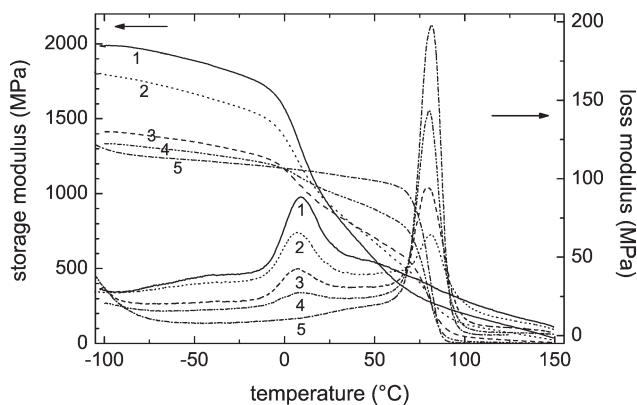


**Figure 4** Effect of the composition (in wt %) of the PP/COC blends on the temperature dependence of the storage modulus  $E_b'$  and of the loss modulus  $E_b''$ . PP/COC = 100/0 (1—full line); 75/25 (2—dotted line); 50/50 (3—dashed line); 25/75 (4—dash-dot-dot line); 0/100 (5—dash-dot line).

68°C; these patterns are believed to indicate the inverse proportionality of the relaxation processes present below and above its temperature.<sup>34</sup>

**Modeling of DMTA results**

To confront experimental data at selected temperatures with the model predictions, we will use a predictive format based on a combination of an equivalent box model (EBM) and modified equations of the percolation theory used for the evaluation of phase continuity.<sup>35–38</sup> The EBM for binary blends in Figure 5 operates with partly parallel (subscript *p*) and partly series (subscript *s*) couplings of components. The EBM is a two-parameter model as of four volume fractions  $v_{ij}$  only two are independent; its volume fractions are interrelated as follows:

$$v_p = v_{1p} + v_{2p}; v_s = v_{1s} + v_{2s}; (v_1 = v_{1p} + v_{1s}; v_2 = v_{2p} + v_{2s}) v_1 + v_2 = v_p + v_s = 1 \quad (3)$$

Equations for storage and loss moduli of binary blends were derived in previous articles<sup>26,31</sup>:

$$E_b' = E_1'v_{1p} + E_2'v_{2p} + v_s^2N'/D \quad (4a)$$

$$E_b'' = E_1''v_{1p} + E_2''v_{2p} + v_s^2N''/D \quad (4b)$$

where

$$N' = v_{1s} E_1'(E_2'^2 + E_2''^2) + v_{2s} E_2'(E_1'^2 + E_1''^2) \quad (5a)$$

$$N'' = v_{1s} E_1''(E_2'^2 + E_2''^2) + v_{2s} E_2''(E_1'^2 + E_1''^2) \quad (5b)$$

$$D = (v_{1s} E_2' + v_{2s} E_1')^2 + (v_{1s} E_2'' + v_{2s} E_1'')^2 \quad (5c)$$

As the EBMs are not self-consistent models, the volume fractions  $v_{ij}$  are to be calculated by using another appropriate model, e.g., modified equations<sup>35–38</sup> based on the percolation theory.<sup>39,40</sup>

$$v_{1p} = [(v_1 - v_{1cr}) / (1 - v_{1cr})]^q, \quad (6a)$$

$$v_{2p} = [(v_2 - v_{2cr}) / (1 - v_{2cr})]^q \quad (6b)$$

where  $v_{1cr}$  or  $v_{2cr}$  is the critical volume fraction (the percolation threshold) at which the component 1 or 2 becomes partially continuous, and  $q$  is the critical exponent.<sup>39</sup> Remaining  $v_{1s}$  and  $v_{2s}$  are evaluated by using eq. (3). In the marginal zone  $0 < v_1 < v_{1cr}$  (or  $0 < v_2 < v_{2cr}$ ), where only component 2 (or 1) is continuous, simplified relations can be used for the minority component, i.e.,  $v_{1p} = 0$  and  $v_{1s} = v_1$  (or  $v_{2p} = 0$  and  $v_{2s} = v_2$ ), to obtain an approximate prediction of mechanical properties. Values of  $q$  are usually located in an interval of 1.6–2.0, so that  $q = 1.8$  can be used also as an average value. For three-dimensional cubic lattice, the percolation threshold  $v_{cr} = 0.156$  was calculated.<sup>41–43</sup> In general, the patterns predicted by using “universal” inputs, i.e.,  $v_{1cr} = v_{2cr} = 0.156$  and  $q = 1.8$ , may not be in a good accord with experimental data because real  $v_{1cr}$  and  $v_{2cr}$  of polymer blends may differ from 0.156 and/or from each other. Their actual values can then be obtained by a fitting procedure, which makes the EBM a valuable source of quantitative information on the phase structure of studied blends.

The effect of the blend composition on  $E_b'$  and  $E_b''$  is confronted with the model predictions in Figure 6: experimental data were extracted from Figure 4, and the universal inputs were used in eqs. (4a) and (4b) (the effect of the composition-dependent PP crystallinity given in Table I was not encompassed because the

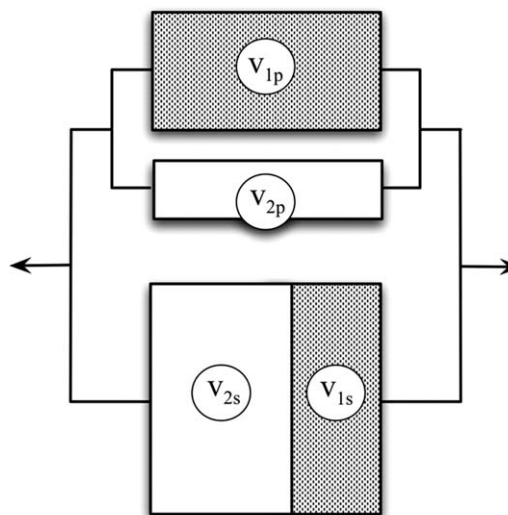


**Figure 5** Equivalent box model for a binary blend 50/50 (schematically).

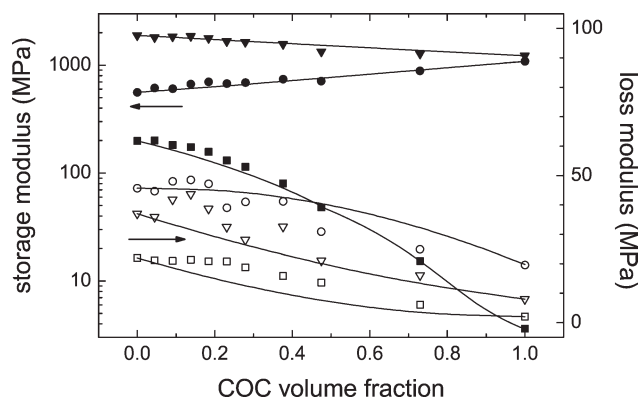


**Figure 6** Effect of the composition (in vol %) of the PP/COC blends on the storage modulus  $E_b'$  (full points) and loss modulus  $E_b''$  (empty points) read at the temperature  $-50^\circ\text{C}$  (triangles),  $50^\circ\text{C}$  (circles) or  $100^\circ\text{C}$  (squares). Full lines: prediction of Eq. (4a) for “universal” input data  $v_{1cr} = v_{2cr} = 0.156$  and  $q = 1.8$ .

dependence of PP modulus on PP crystallinity could not be estimated). The prediction of  $E'$  fits the experimental data very well: the graph shows that storage modulus at  $50^\circ\text{C}$  rises with the COC content (which holds for the moduli from the central interval  $25\text{--}75^\circ\text{C}$ ), whereas the modulus at  $-50^\circ\text{C}$  or  $100^\circ\text{C}$  decreases. On the other hand, the prediction of  $E''$  at 50 and  $100^\circ\text{C}$  seems to be partially underestimated, and the results may be considered plausible taking into account a mild stiffening effect of microfibrers.

Moreover, Figure 7 shows that the maxima of the loss modulus  $E_{bm}''$  (PP) and  $E_{bm}''$  (COC), taken as the height of the respective peaks, are in a good accord with the prediction of eq. (4b). It is worth noting that tensile modulus of the blends observed in the stress–strain measurements in the direction of injection molding (i.e., produced fibers of COC) rather followed the rule of mixtures in the composi-

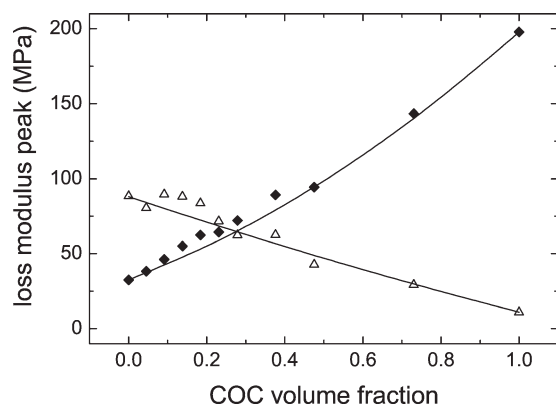


**Figure 7** Effect of the composition (in vol %) of the PP/COC blends on the maximum  $E_{bm}''$  of the loss modulus read off for the glass transition peaks of PP (open triangles) and COC (solid diamonds), respectively. Full lines: prediction of eq. (4b) for “universal” input data  $v_{1cr} = v_{2cr} = 0.156$  and  $q = 1.8$ .

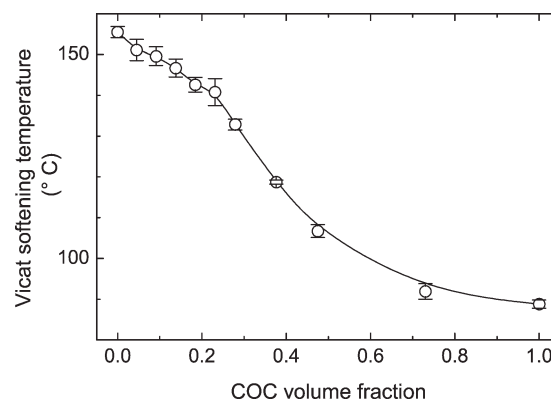


**Figure 8** Effect of the composition (in vol %) of the PP/COC blends on the Vicat softening temperature (10N,  $120^\circ\text{C}/\text{h}$ ; ASTM D1525-09).

tion interval 10–40% COC.<sup>11</sup> It seems that DMTA performed in bending mode at very small deformations cannot differentiate between structures encompassing COC fibers or COC cocontinuous phase.

#### Vicat softening temperature

The VST of PP, measured at  $120^\circ\text{C}/\text{h}$  and 10N,  $VST = 155 \pm 1^\circ\text{C}$  (Fig. 8), is in a good agreement with the literature data for analogous grade PP.<sup>44</sup> On the other hand,  $VST = 89 \pm 1^\circ\text{C}$  of COC is higher than  $VST = 80^\circ\text{C}$  reported in Technical Data Sheet, however for more critical testing conditions ( $50^\circ\text{C}/\text{h}$ , 50N).<sup>45</sup> In this context, it is worth noting that the experimental standard deviation of VST in our measurements ranges between 1 and  $3^\circ\text{C}$ . The PP/COC blends show a virtually linear decrease in VST with the COC volume fraction in the interval  $0 < v_2 < 0.23$ , whereas at higher COC fractions, a steeper decrease is observed.

Bastida et al.<sup>46</sup> proposed VST as a method suitable for assessment of the phase behavior. They revealed that two-component blends of immiscible glassy polymers show a typical S-shaped decrease in VST as a function of the blend composition, if two distinct phases are present. The behavior of our PP/COC blends (Fig. 8), which undoubtedly consist of two distinct components, is in full conformity with this finding.<sup>15</sup> Analogous dependences of VST on the blend composition were published for blends consisting a semicrystalline polymer and an amorphous glassy polymer, i.e., polyoxymethylene/phenoxo,<sup>47</sup> polyamide/polyvinyl chloride (PVC),<sup>48</sup> and polybutyleneterephthalate/polyamino-ether.<sup>49</sup> In all cases, the initial linear decrease (up to about  $v_2 = 0.3\text{--}0.4$ ) in VST can be attributed to the softening of the majority semicrystalline component. In the composition range where glassy amorphous polymer becomes the dominating phase, whereas semicrystalline component loses its phase continuity, a steeper

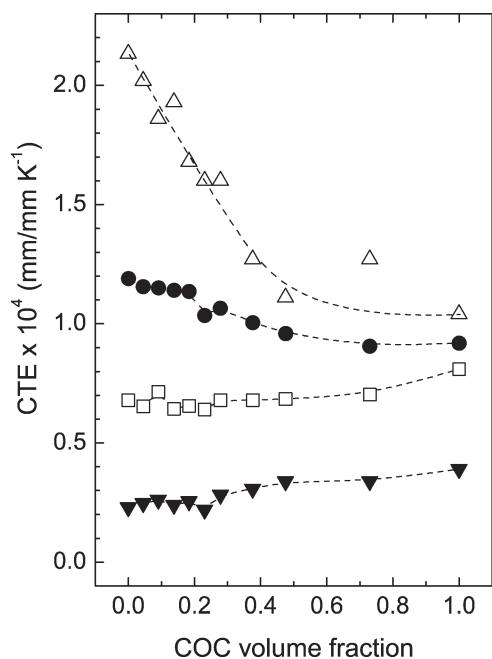


**Figure 9** Coefficient of linear thermal expansion (CLTE) as a function of the PP/COC blend composition. Average values read off in the following temperature intervals:  $-40$  to  $-20^{\circ}\text{C}$  ( $\blacktriangle$ );  $-20$  to  $20^{\circ}\text{C}$  ( $\square$ );  $20$ – $40^{\circ}\text{C}$  ( $\bullet$ );  $40$ – $70^{\circ}\text{C}$  ( $\triangle$ ).

VST decrease was observed. Thus, we can say that the dependence of VST on the composition of the PP/COC blends is in a good conformity with our morphological analysis.<sup>15</sup>

### Coefficient of linear thermal expansion

The CLTE was evaluated for four temperature intervals in the range between  $-40$  and  $70^{\circ}\text{C}$  as specified in Figure 9. The value of CLTE for neat PP increases with temperature from  $0.25 \times 10^{-4} \text{ K}^{-1}$  at  $-30^{\circ}\text{C}$  to  $1.20 \times 10^{-4} \text{ K}^{-1}$  at  $30^{\circ}\text{C}$  and  $2.10 \times 10^{-4} \text{ K}^{-1}$  at  $55^{\circ}\text{C}$ , whereas COC is characterized by values  $0.35 \times 10^{-4} \text{ K}^{-1}$ ,  $0.85 \times 10^{-4} \text{ K}^{-1}$ , and  $0.90 \times 10^{-4} \text{ K}^{-1}$ , respectively. These data are in a good agreement with the values reported in the literature for the room temperature, i.e.,  $1.00 \times 10^{-4} \text{ K}^{-1}$  for PP and  $0.70 \times 10^{-4} \text{ K}^{-1}$  for COC.<sup>6,50</sup> CLTEs found for the temperature intervals  $-40$  to  $-20^{\circ}\text{C}$  and  $-20$  to  $20^{\circ}\text{C}$  are almost independent of the composition of the blends containing  $0 < v_2 < 0.3$  of COC, which indicates the dominating effect of the PP component. For  $v_2 > 0.3$ , a small linear increase in CLTE with the fraction of COC indicates the rising role of the COC cocontinuity. In the interval  $20$ – $40^{\circ}\text{C}$ , which is located above the glass transition of PP, a virtually linear decrease in CLTE with the fraction of COC can be observed. Finally, in the interval  $40$ – $70^{\circ}\text{C}$ , a steep decrease in CLTE with the COC fraction characterizes the blends in the region  $0 \leq v_2 \leq 0.50$ ; for  $v_2 \approx 0.5$ ,  $\text{CLTE} = 1.27 \times 10^{-4} \text{ K}^{-1}$  may be associ-

ated with the higher percentage of amorphous PP in these blends. It should be noted that above  $80^{\circ}\text{C}$ , the injection molded specimens of the PP/COC 25/75 blend and COC exhibited an increasing tendency to shrinking when  $T_g$  of the major component was exceeded.

Alternatively, Figure 10 shows CLTEs of PP, COC, and two selected blends as functions of temperature. The plotted curves,  $\text{CLTE}(T)$ , were obtained as the derivative  $D(T)$  of the polynomial function fitting the length variation  $\Delta L(T)$  with temperature, according to eq. (7)

$$\text{CLTE}(T) = [\Delta L(T)/\Delta T]/L_0 = D(T)/L_0 \quad (7)$$

where  $L_0$  is the initial specimen length.  $\text{CLTE}(T)$ s of all materials are very similar in the interval between  $-40$  and  $0^{\circ}\text{C}$ , i.e., up to the glass transition temperature of PP. Both PP and the 75/25 blend show a steep rise of  $\text{CLTE}(T)$  above  $0^{\circ}\text{C}$  from about  $0.6 \times 10^{-4} \text{ K}^{-1}$  to about  $2.2$ – $2.7 \times 10^{-4} \text{ K}^{-1}$  at  $70^{\circ}\text{C}$ . On the other hand,  $\text{CLTE}(T)$  of the blends with  $v_2 \geq 0.4$  can be expected to lie in a relatively narrow interval delimited by the dependencies for PP/COC = 50/50 and COC. It is evident that more pronounced dilatation is typical of the PP-rich blends.

### CONCLUSIONS

Morphology and interfacial interaction of the injection molded PP/COC immiscible blends were found to markedly affect their physical properties. Observed  $T_g$ s of the blend components are independent of the blend composition. Density measurements evidence the volume additivity of components, which is in conformity with the immiscibility of PP and COC. The melting temperature of PP in the blends slightly

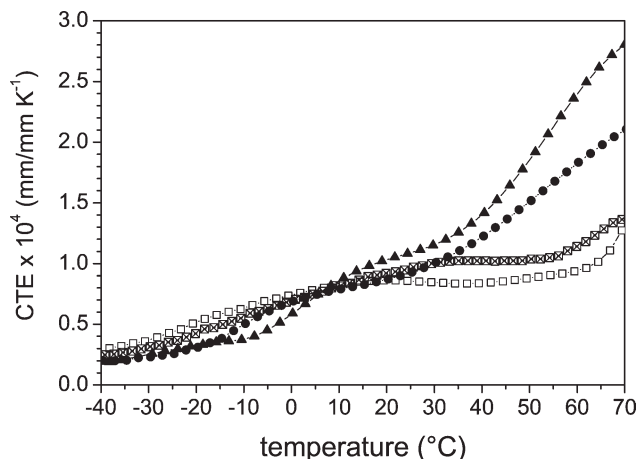


**Figure 10** Coefficient of linear thermal expansion (CLTE) as a function of temperature. PP/COC = 100/0 ( $\blacktriangle$ ); 75/25 ( $\bullet$ ); 50/50 ( $\boxtimes$ ); 0/100 ( $\square$ ).

decreases at COC volume fraction higher than 0.4, which indicates augmentation of imperfections in the PP crystalline phase. The crystallization temperature of PP in blends observed in the cooling scan is 2–5°C higher than that of the neat PP, which might indicate a tiny nucleating effect of COC. Parallel declines in the melting temperature, crystallization temperature, and crystallinity of PP found for the 25/75 blend indicate that the dominating COC component inhibits the structural organization in the PP component and induces a fractionated crystallization.

The effect of the blend composition on the storage modulus and loss modulus is in a plausible accord with the simultaneous prediction based on the predictive scheme operating with a two-parameter EBM and the data on the partial phase continuity of the components obtained from modified equations of the percolation theory. The dependence of the VST on the blend composition is typical of immiscible blends and is in good conformity with the morphological analysis. The CLTE evaluated as a function of blend composition or temperature reveals that the blend expansion (i) is controlled by the fraction and cocontinuity of the components, (ii) is more pronounced for the PP-rich blends, and (iii) generally rises with temperature.

The authors are very much obliged to Dr. *Paolo Goberti* (Lyondell-Basell, Italy) for the blend preparation, and to *Lyondell-Basell* (Italy) and *TOPAS Advanced Polymers* (Germany) for kind supply of PP and COC, respectively.

## References

- Mc Nally, D. *Modern Plastics World Encyclopedia*; Hightstown: NJ, 2001, p B8.
- Tritto, I.; Boggioni, L.; Jansen, J. C.; Thorshaug, K.; Sacchi, M. C.; Ferro, D. R. *Macromolecules* 2002, 35, 616.
- Thorshaug, K.; Mendichi, R.; Boggioni, L.; Tritto, I.; Trinkle, S.; Friedrich, C.; Muelhaupt, R. *Macromolecules* 2002, 35, 2903.
- Mc Nally, D. In *Encyclopedia of Polymer Science and Technology*, 3rd ed.; Mark, H. F., Ed.; Wiley: Hoboken, NJ, 2003; Vol.2, p 489.
- Chu, P. P. J.; Huang, W. J.; Chang, F. C. *Polymer* 2001, 42, 2185.
- TOPAS Advanced Polymers GmbH, TOPAS COC product overview (*topas\_brochure\_english.pdf*). Available at: [www.topas.com/news-literature-brochures](http://www.topas.com/news-literature-brochures). Accessed December 2010.
- Scrivani, T.; Benavente, R.; Perez, E.; Perena, J. M. *Macromol Chem Phys* 2001, 202, 2547.
- Forsyth, J. F.; Scrivani, T.; Benavente, R.; Marestin, C.; Perena, J. M. *J Appl Polym Sci* 2001, 82, 2159.
- Khanarian, G. *Polym Eng Sci* 2000, 40, 2590.
- Kolarik, J.; Pegoretti, A.; Fambri, L.; Penati, A. *Macromol Mater Eng* 2003, 288, 629.
- Pegoretti, A.; Kolarik, J.; Fambri, L.; Penati, A. *Polymer* 2003, 44, 3381.
- Utracki, L. A. *Polymer Alloys and Blends*; Hanser Publ: Munich, 1990.
- Rana, D.; Lee, C. H.; Cho, K.; Lee, B. H.; Choe, S. *J Appl Polym Sci* 1998, 69, 2441.
- Luettmmer-Strathmann, J.; Lipson, J. E. G. *Macromolecules* 1999, 32, 1093.
- Slouf, M.; Kolarik, J.; Fambri, L. *J Appl Polym Sci* 2004, 91, 253.
- Fambri, L.; Kolarik, J.; Pasqualini, E.; Penati, A.; Pegoretti, A. *Macromol Symp* 2008, 263, 114.
- Kim, B. K.; Do, I. H. *J Appl Polym Sci* 1996, 60, 2207.
- Afshari, M.; Kotek, R.; Kish, M. H.; Dast, H. N.; Gupta, B. S. *Polymer* 2002, 43, 1331.
- Li, Z. M.; Yang, W.; Li, J. B.; Xie, B. H.; Huang, R.; Yang, M. B. *J Polym Sci B: Polym Phys* 2003, 42, 374.
- Li, Z. M.; Yang, W.; Xie, B. H.; Shen, K. Z.; Huang, R.; Yang, M. B. *Macromol Mater Eng* 2004, 289, 349.
- Xing, Q.; Zhu, M.; Wang, Y.; Chen, Y.; Zhang, Y.; Pionteck, J.; Adler, H. *J Polymer* 2005, 46, 5406.
- Fallahi, E.; Barmar, M.; Kish, M. H. *J Appl Polym Sci* 2008, 108, 1473.
- Xue, C. H.; Wang, D.; Xiang, B.; Chiou, B. S.; Sun, G. *J Polym Sci B: Polym Phys* 2010, 48, 921.
- Goitisoló, I.; Eguiazabal, J. I.; Nazabal, J. *Macromol Mater Eng* 2010, 295, 233.
- Howe, D. V. I. *Polymer Data Handbook*; Mark, J. E., Ed.; Oxford University Press: New York, 1999; p 780.
- Kolarik, J.; Krulis, Z.; Slouf, M.; Fambri, L. *Polym Eng Sci* 2005, 45, 817.
- Frensch, H.; Harnischfeger, P.; Jungnickel, B. J. In *Multiphase Polymers: Blends and Ionomer*; Utracky, L. A., Weiss, R. A., Eds.; ACS Symp Ser 1989; Vol.395, Chapter 5, p 101.
- Arnal, M. L.; Muller, A. J.; Maiti, P.; Hikosaka, M. *Macromol Chem Phys* 2000, 201, 2493.
- Wang, K.; Zhou, C.; Yu, W. *J Appl Polym Sci* 2002, 85, 92.
- Pimbert, S. *Macromol Symp* 2003, 203, 277.
- Kolarik, J.; Fambri, L.; Slouf, M.; Konecny, D. *J Appl Polym Sci* 2005, 96, 673.
- Dorigato, A.; Pegoretti, A.; Fambri, L.; Lonardi, C.; Slouf, M.; Kolarik, J. *Express Polym Lett* 2011, 5, 23.
- Bai, F.; Li, F.; Calhoun, B. H.; Quirk, R. P.; Cheng, S. Z. D. In *Polymer Handbook*; 4th ed.; Brandrup, J., Immergut, E. H., Grulke, E. A., Eds.; J Wiley & Sons: Hoboken, NJ, 1999; p V-24.
- Kolarik, J. *Adv Polym Sci* 1982, 46, 119.
- Kolarik, J. *Polym Networks Blends* 1995, 5, 87.
- Kolarik, J.; Fambri, L.; Pegoretti, A.; Penati, A. *Polym Eng Sci* 2000, 40, 127.
- Kolarik, J. *J Macromol Sci Phys* 2000, 39, 53.
- Kolarik, J.; Pegoretti, A.; Fambri, L.; Penati, A. *J Appl Polym Sci* 2003, 88, 641.
- De Gennes, P. G. *J Phys Lett (Paris)* 1976, 37, 1.
- Lyngaae-Jorgensen, J.; Kuta, A.; Sondergaard, K.; Poulsen, K. V. *Polym Networks Blends* 1993, 3, 1.
- Utracki, L. A. *J Rheol* 1991, 35, 1615.
- Sax, J.; Ottino, J. M. *Polym Eng Sci* 1983, 23, 165.
- Hsu, W. Y.; Wu, S. *Polym Eng Sci* 1993, 33, 293.
- MatWeb, Polypropylene Homopolymer. Available at: [www.matweb.com](http://www.matweb.com). Accessed December 2010.
- TOPAS Advanced Polymers GmbH, Technical Datasheet of Topas 8007S-04. Available at: [www.topas.com/tech-services-technical-datasheets](http://www.topas.com/tech-services-technical-datasheets). Accessed December 2010.
- Bastida, S.; Eguiazabal, J. I.; Nazabal, J. *Polymer Test* 1993, 12, 233.
- Erro, R.; Gaztelumendi, M.; Nazabal, J. *J Polym Sci B: Polym Phys* 1996, 32, 1055.
- Lian, Y.; Zhang, Y.; Peng, Z.; Zhang, X.; Fan, R.; Zhang, Y. *J Appl Polym Sci* 2001, 80, 2823.
- Granado, A.; Eguiazabal, J. I.; Nazabal, J. *J Appl Polym Sci* 2004, 91, 132.
- Dominghaus, H. *Plastics for Engineers: Materials, Properties, Applications*; Carl Hanser Verlag: Munich, 1993; p 86.